Optical Test Results of Fast pnCCDs

Sebastian Ihle, Robert Hartmann, Marc Downing, Lothar Strüder, Sebastian Deiries, Hubert Gorke, Sven Hermann, Gottfried Kanbach, Janis Papamasturakis, Heike Soltau, and Alexander Stefanescu

***Abstract*—Measurements with a high-speed pn-charge coupled device (pnCCD) system have been performed in the optical and near infrared (NIR) wavelength range. Some of the key parameters of the system that were determined include the overall quantum efficiency (QE), the point spread function (PSF) and the photon transfer curve (PTC). The results of these measurements will be presented below. The measurements have been carried out at the optical test bench of ESO in Garching, Germany. There we also demonstrated for the first time the feasibility of a fast readout scheme that allows the system to be operated at a speed of up to 1000 frames per second (fps) for use with optical light. Additionally astronomical test measurements have been performed at the Skinakas telescope on Crete, Greece.**

***Index Terms*—pnCCD, high-speed, quantum efficiency, photon transfer curve**

I. Introduction

FUTURE instruments for adaptive optics (AO) systems at current $10\,\mathrm{m}$ class telescope facilities and the planned extremely large telescopes (ELT) require new detector systems. They need large pixel arrays (256×256 pixels or more) because future deformable mirrors will use several thousand actuators for the corrections of wavefronts. The required frame rate will rise to more than 1000 fps to correct fast variations of atmospheric turbulence. Since the natural or artificial guide stars have a limited brightness the low signal per frame requires very low readout noise to accurately determine the necessary corrections. For the same reason the QE at the used wavelengths should be as high as possible.

Similar requirements arise in the relatively new field of High Time Resolution Astronomy. While observing the fast light intensity variations of the examined object, a large pixel array makes it possible to have sources with known magnitudes in the same field of view. This allows to perform relative differential photometry by comparing the brightness of several objects. Many interesting sources are rather faint which also implies demanding requirements for readout noise and QE especially in the NIR.

S. Ihle, e-mail: (sebastian.ihle@pnsensor.de), R. Hartmann and H. Soltau are with the company PNSensor GmbH, Otto-Hahn-Ring 6, 81739 München, Germany and the Semiconductor Laboratory of the Max-Planck-Institutes, München.

M. Downing and S. Deiries are with ESO, the European Organisation for Astronomical Research in the Southern Hemisphere, Garching, Germany.

L. Strüder is with the Max-Planck-Institut für extraterrestrische Physik, Garching, Germany, the Semiconductor Laboratory of the Max-Planck-Institutes, München, Germany and the Universität Siegen, Germany.

H. Gorke is with the Forschungszentrum Jülich, Germany.

S. Hermann, G. Kanbach and A. Stefanescu are with the Max-Planck-Institut für extraterrestrische Physik, Garching, Germany.

J. Papamasturakis is with the University of Crete, Heraklion, Greece.

Manuscript received November 14, 2008.

At the Semiconductor Laboratory of the Max-Planck-Institutes a pnCCD system was developed for such applications together with the company PNSensor. Its performance was measured at the optical test bench of ESO. The system also includes a data acquisition system that can handle the enormous data rates that arise. First a description of the system and its components is given. Then the performed measurements and results are presented.

II. The pnCCD system for optical applications

A. The pnCCD principle

The pnCCD is a pnp-structure that is based on the principle of sideward depletion. It is fabricated from high purity n-type silicon. The back side, that consists of an unstructured, ultra-thin p^+-implantation, is used as entrance window for photons. On the front side the transfer registers are formed by p^+-implantations. By application of adequate voltages to the rear and the frontside the full detector volume is depleted [1]. The potential minimum for electrons is thereby formed close to the front side. There the electrons are collected in the pixels formed by the implantations. After integration the electrons can be shifted towards the readout anode using the three transfer registers. A schematical cut through one channel of the detector is shown in figure 1.

Due to the fully depleted substrate and the thin entrance window the whole detector volume of $450\,\mu\mathrm{m}$ thickness is sensible to incident radiation. This results in highly improved QE in the NIR compared to thin CCDs as well as an effective suppression of fringing effects. Also the homogeneous entrance window gives a fill factor of 100 %. By implementing additional dielectric layers on top of the silicon an optical anti-reflective coating (ARC) can be created [2]. Such an ARC increases the QE over the whole optical and NIR regime significantly. The properties of the ARC can be tailored to the requirements given by the application.

The pnCCD that we used for the described optical measurements has an image area of 264×264 pixels with $48 \times 48\,\mu\mathrm{m}^2$ pixel size, altogether $12.7 \times 12.7\ \mathrm{mm}^2$. The charge transfer inefficiency is as low as 10^{-5}. The pixel full well capacity is about 10^5 electrons which is much higher than needed by any optical high-speed application.

B. The detector readout

The pnCCD features split-frame transfer, i.e. the image area is split into halves and read out to opposite directions. Next to each half is a frame store area of equal size. A schematic of the pnCCD and its readout ASICs is shown in figure 2.

Photons that are incident on the image area during transfer are registered as signal in a wrong pixel. To minimize these

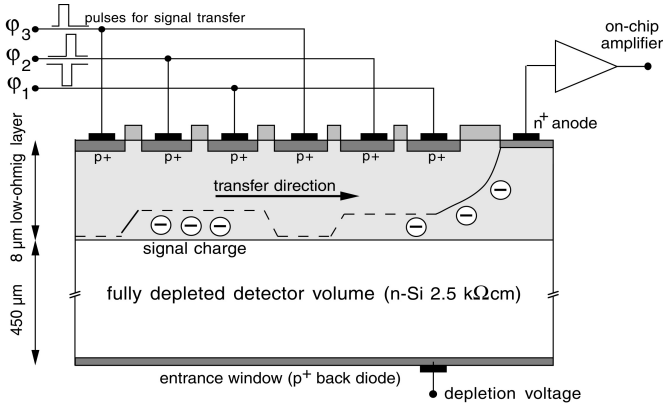

Fig. 1. Schematic cross-section of the fully depleted pnCCD. The full detector volume is sensible to radiation. The signal electrons are collected in a layer several µm beneath the device frontside. By application of pulses to the transfer registers the signal is shifted to the readout anode of each channel which is connected to its own on-chip JFET amplifier.

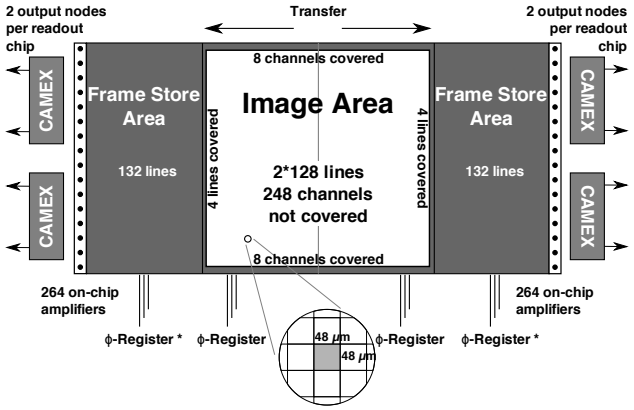

Fig. 2. Schematic illustration of the pnCCD with the CAMEX readout chips. The light sensitive image area is split into halves. Next to each half are the two frame store areas. Both frame stores as well as two times 8 reference channels and 4 reference lines in the image area are covered by an aluminum layer. Each channel has an on-chip JFET amplifier which is wire bonded to the CAMEX chips which perform column-parallel amplification.

out-of-time events the image is shifted very rapidly into the frame store and read out from there instead. The frame store areas are shielded by an aluminum layer against optical light. This fast transfer takes only about 30 µs. The frame stores are read out in parallel via one on-chip JFET amplifier per channel. Every amplifier is wire bonded to the readout ASICs called CAMEX (CMOS Amplifier and MultiplEX) chip with 132 channels each. Therefore no serial register is needed on the pnCCD.

The CAMEX chips perform column-parallel amplification. They feature multi correlated double sampling (MCDS) with up to eight-fold sampling. A sample and hold stage allows multiplexing of the signals to two output nodes per chip simultaneous to the amplification of the next line. Different amplification gains can be chosen by programming. At normal speed operation both amplifiers of each channel are reset before the readout of every line. For high-speed applications with low light levels Hartmann et al. [2] proposed a novel readout scheme for our CAMEX chips. Thereby the first amplifier is not reset for every line. The baseline, which is usually given by zero signal, is then the signal level of the previous pixel. With this optimized MCDS scheme the noise properties remain practically unchanged. However, apparently the internal voltage of the amplifier increases with the total signal. This limits the total number of electrons that can be measured without performance decrease to about 6000 per channel at highest gain. With this fast readout mode the pnCCD system can be operated with a speed of up to 1000 fps. This corresponds to about 70 MHz mean pixel rate.

In X-ray applications it can often be assumed that only few pixels contain signal. By use of intelligent algorithms all channels can be used for common-mode variations, offset variations that are common to a whole line. For many optical applications such an assumption cannot be made. Therefore in the image area 8 reference channels on each border of the pnCCD are shielded by an aluminum layer. The central 6 of which can safely be assumed to contain no signal. They can therefore be used for correction of common-mode variations. At a typical operation temperature of about -55 °C the overall noise of the pnCCD system is less than 2.3 electrons equivalent noise charge (ENC) when all channels can be used for correction. The use of only 6 channels increases the noise by about 8 % to 2.4 electrons ENC.

III. Measurement results

The measurements of the detector parameters have been performed at the optical test bench of ESO in Garching, Germany. The main feature of the test bench is to illuminate the detector homogeneously with light. Alternatively, a point-like illumination with a tiny focused light spot can be applied.

The light source of the test bench is a halogen lamp that produces a thermal light spectrum. A double monochromator is used to suppress the light outside a chosen band with a minimum bandwith of 3 nm and a central wavelength between 300 nm and 1100 nm. The monochromatic light is optionally attenuated by a set of neutral density filters. It is then either fed into a fiber or transmitted into an integrating sphere.

The fiber guides the light to a position a few centimeters in front of the detector where a small optic focuses the light through the window of the vacuum chamber to a tiny spot of 2 µm diameter on the entrance window of the detector. The fiber end including the focusing optics can be moved in all three dimensions by a translation stage to adjust the focus and the position of the spot. This can be used to measure the PSF of the pnCCD.

The integrating sphere diffuses the light. The distance of the output port of the integrating sphere and the entrance window of the vacuum chamber is about half a meter. Therefore the illumination of the detector with its size of about 15 mm can safely be assumed homogeneous.

A. Quantum efficiency

The overall QE of a detector can be determined by measuring how many photons can be detected compared to a known number of incident photons. The ESO test bench includes a photo diode to measure the light intensity in the integrating

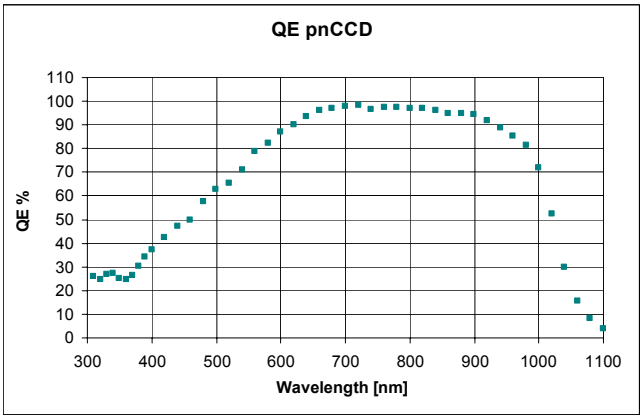

Fig. 3. Measured QE in the wavelength range from 300 nm to 1100 nm. The pnCCD featured an ARC optimized for red and NIR wavelengths. The QE is high over a wide wavelength range and peaks at almost 100 %.

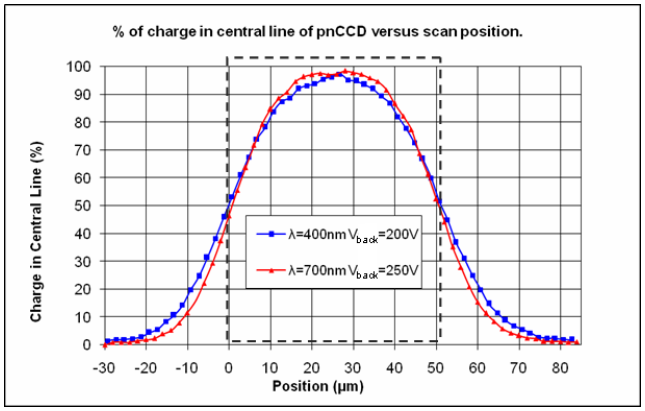

Fig. 4. For the measurement of the PSF a tiny spot of light was projected onto the detector and moved in small steps. At every position one image was taken. Plotted is the measured signal in one line compared to the total signal in a surrounding region. The measurements were performed for two different back contact voltages. The pixel size is visualized by the dashed rectangle.

sphere. The whole system is calibrated such that with the measured photodiode current the photon flux can be calculated in the plane of the detector.

To convert a signal measured by a detector system in ADU into the number of detected photons the gain in ADU per electron has to be known. For our pnCCD system the gain has been measured by two independent methods. On the one hand calibration with X-rays was performed at the Semiconductor Laboratory of the Max-Planck-Institutes. The pnCCD was illuminated by a ^{55}Fe source that emits the ^{55}Mn K_α line with an energy of 5.9 keV. On the other hand the gain was determined from PTC measurements (see section III-C). Furthermore it has been shown that every photon that is absorbed in a pnCCD creates one electron that is then registered [3].

Homogeneously illuminated images have been taken with light of wavelength ranging from 300 nm to 1100 nm. Similar mean signals were applied by adjusting the used attenuation filter and the integration time of the images. The QE values that have been derived are shown in figure 3. The pnCCD used for the measurement has an ARC that is optimized for the red and NIR wavelength range. As result the measurement shows high QE at these wavelength, peaking at almost 100 %. This result is in good accordance with previous measurements [2].

B. Point spread function

The PSF is a measure of the spatial resolution of CCDs for point-like illumination. The application of point-like objects is given e.g. in imaging astronomy or for Shack-Hartmann wavefront sensors for AO systems at optical telescopes.

The PSF is measured using the so called virtual knife-edge method [4]. For this a point like spot is projected onto the detector. While the spot is moved over the detector in small steps one image is taken for each position. A virtual region of pixels for the analysis is chosen such that the spot is initially outside and at the end entirely inside. The edge of the region can be regarded as a “virtual knife-edge”. In the analysis the total signal inside the region compared to the total signal of a larger surrounding region is measured depending on the spot position.

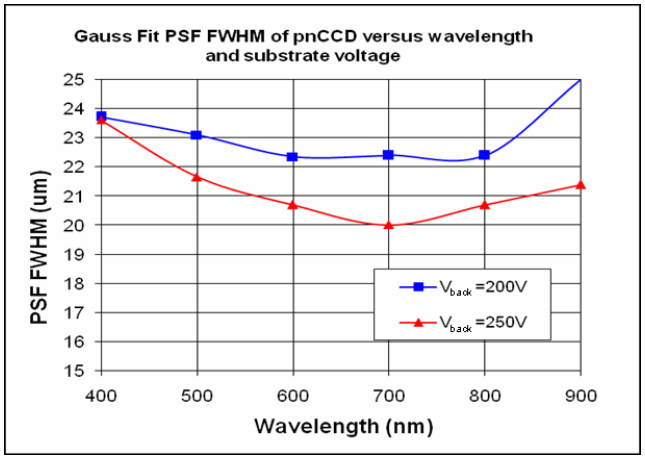

Fig. 5. Shown are the FWHM values of Gaussian fits to the derivative of the collected charge in the analysis region over the spot position for several different wavelengths and two different depletion voltages. The measured PSF is as low as 20 µm FWHM or 8.5 µm rms.

Figure 4 shows the signal in a region that consists of only one line. At the two edges of the pixel (marked by the dashed rectangle) half of the signal is inside the region as expected. In the center of the pixel almost all signal is collected in the examined pixel.

The charge collected inside the analysis region in dependence of the spot position is described by an error function. The derivative of this function with respect to the position is a Gaussian function. The width of the PSF can be determined by a fit to either of both functions. The results of the Gaussian fits for measurements at several different wavelength and two different depletion voltages are shown in figure 5. At 700 nm the PSF is as low as 20 µm FWHM or 8.5 µm rms. This value is in good accordance with mesh measurements performed with X-rays [5]. Considering the detector thickness of 450 µm this is a very good value.

For wavelength longer than 700 nm the measured PSF is increasing. This is probably due to the increasing penetration depth of light at these wavelength and the divergence of the focused light beam. The increase for shorter wavelength is still

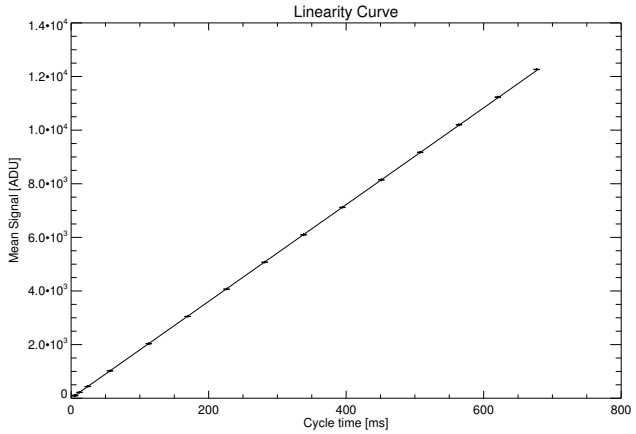

Fig. 6. Linearity of the pnCCD system at maximum gain at a nominal frame rate of about 300 fps. The measured mean signal is plotted versus the cycle time.

under investigation.

The measured width of the PSF is clearly smaller than half the pixel size. It is therefore more than a factor of two smaller than demanded by ESO for future AO applications.

C. Photon transfer curve

The PTC is a standard method to measure the linearity of a CCD system. The method evaluates the response of the CCD system for different illuminations. Usually a constant integration time is used. The intensity of the light source is increased or a mechanical shutter is used to control the illumination time. The use of a mechanical shutter is not feasible because of the short integration times we often operate our system with. Also the test setup at ESO can only change the intensity of the light in large steps. Therefore we change the integration time of the pnCCD to achieve the required different illuminations.

To measure the PTC of the pnCCD a constant illumination is applied and a series of measurements with increasing integration time is performed. For accurate results the temporal stability of the light source is important. This was checked by the photo diode in the setup. The level of illumination is chosen such that the whole dynamic range of the system at a given gain can be probed with a maximum integration time of less than one second. All measurements were performed at a nominal frame rate of about 300 fps. This means that the whole pnCCD is read out in a bit more than 3 ms independent of the integration time.

The cycle time is the sum of integration time and the time needed for readout. It is the time interval for which every pixel is exposed to light. An internal clock of the system tags every image with a timestamp that can be used to derive the cycle time. Since it is proportional to the mean number of photons incident on any pixel the measured mean signal over the image should ideally show a linear dependence on it (see figure 6). The non-linearity is plotted in figure 7 as the percentaged deviation from a fitted line through origin. The non-linearity is better than half a percent for the whole dynamic range.

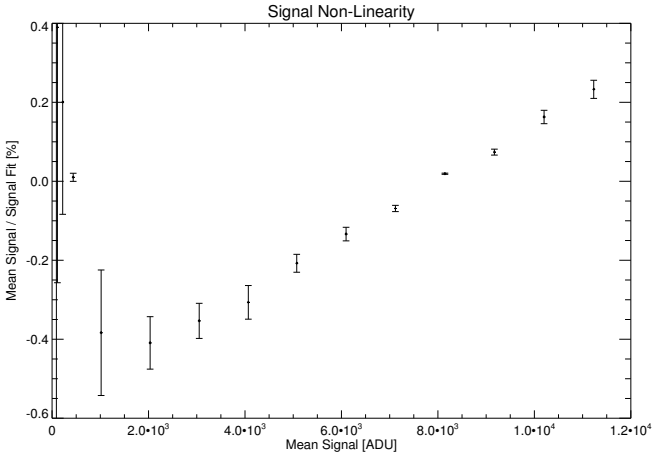

Fig. 7. Non-linearity of the pnCCD system at maximum gain at a nominal frame rate of about 300 fps. Plotted is the percentaged deviation of the measured mean signal from a fitted line through origin. With less than half a percent over the whole dynamic range the system shows an excellent performance.

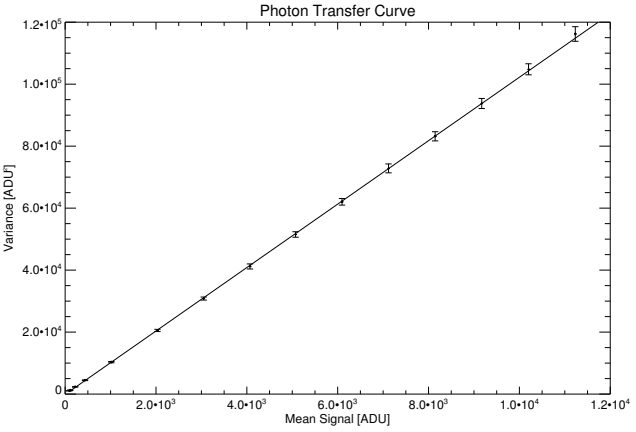

Fig. 8. Photon transfer curve of the pnCCD system at maximum gain at a nominal frame rate of about 300 fps. Plotted is the measured mean variance versus the measured mean signal. The variance of a dark measurement is subtracted. The error bars denote the standard deviation of variance values of 100 measurements. No relevant saturation effects or contributions of fixed pattern noise are visible.

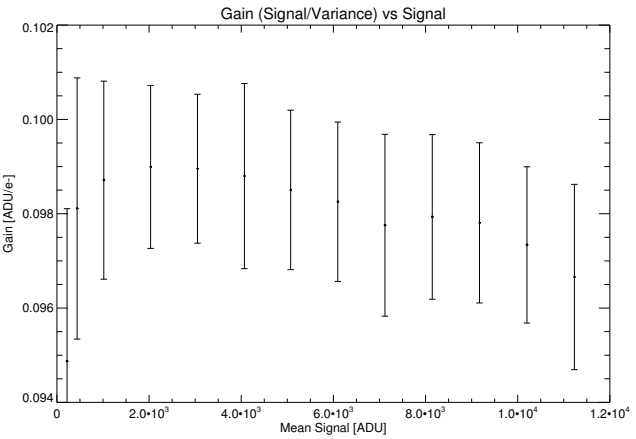

Fig. 9. Gain of the pnCCD system determined from the measured variance and mean signal. The error bars denote the standard deviation of variance values of 100 measurements. The gain is almost constant over the whole dynamic range.

Knowing the reasonable linearity of the system, the actual photon transfer curve can be evaluated. For this purpose the measured variance or the standard deviation of the signal over the examined area of the CCD is plotted versus the measured mean signal. Since the variance is according to photon statistics proportional to the mean number of incident photons there is a linear correlation between the variance and the mean signal.

The variance of the signal over the area of the pnCCD is calculated by subtraction of two images. This removes all offset variations and the mean value of the signal. Only the pixel to pixel signal variations due to photon noise and possibly other noise effects remain. The variance is then directly calculated over the examined area. To remove the readout noise the variance of a dark image is subtracted. In figure 8 the measured PTC for highest gain is shown. According to statistics the variance is a property that exhibits a much larger dispersion than the mean. Therefore the calculations were performed for 100 pairs of images for every illumination level. The error bars in the plot denote the standard deviation.

Deviations from a linear correlation for high signals can indicate saturation effects or fixed pattern noise. Nothing like this is visible here. Also often the full well capacity can be determined from a PTC measurement. This is not possible here since the full well capacity of the pnCCD is by far not reached inside the dynamic range when the highest gain is used.

Additionally the gain can be calculated directly from the PTC measurement. It is the proportionality factor between the measured variance and the measured signal. In figure 9 the calculated gain is plotted versus the mean signal. It can be seen that the gain is almost constant over the whole dynamic range. The value determined this way is in good agreement with X-ray calibration measurements performed at the Semiconductor Laboratory of the Max-Planck-Institutes.

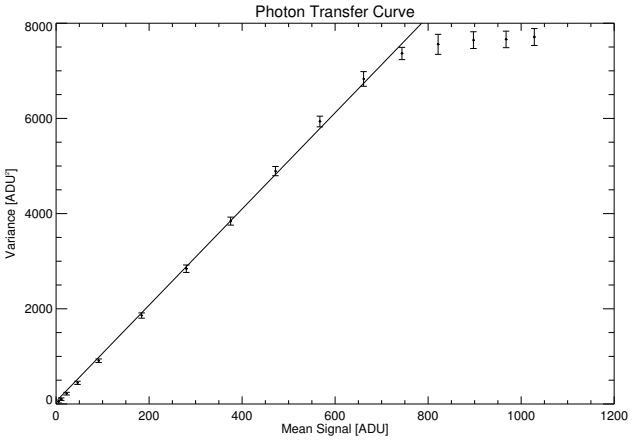

Fig. 10. Photon transfer curve of the pnCCD system operated in the fast readout mode at maximum gain. The nominal frame rate is about 900 fps. Plotted is the measured mean variance versus the measured mean signal. The variance of a dark measurement is subtracted. The error bars denote the standard deviation of variance values of 100 measurements. No relevant saturation effects or contributions of fixed pattern noise are visible.

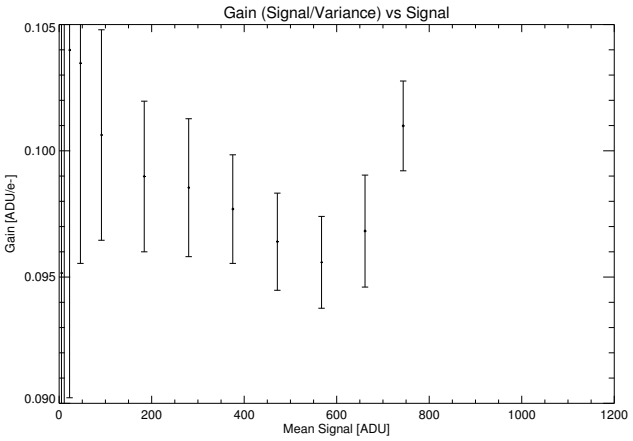

Fig. 11. Gain of the pnCCD system operated in the fast readout mode at maximum gain. It is determined from the measured variance and mean signal. The error bars denote the standard deviation of variance values of 100 measurements. The gain is almost constant over the whole dynamic range.

D. Fast readout mode

For the first time we demonstrated the feasibility of the fast readout scheme described in section II-B for an application with optical light. For this we performed PTC measurements with a nominal frame rate of about 900 fps with the same measurement setup. The overall performance is as good as anticipated.

In figure 10 the PTC curve measured with the fast readout mode is shown. As explained, the amplifier in the CAMEX chip reaches saturation for signals that are too large. The value of 600 ADU corresponding to about 60 electrons per pixel matches well to the predicted value of 6000 electrons per column.

The gain (see figure 11) is equal to the normal speed readout for small signals. For large signals that approach the saturation level the gain drops by a few percent.

IV. Astronomical test measurements

Astronomical test observations were performed at the Skinakas telescope of the University of Crete, Greece. The telescope has a $1.2\,\mathrm{m}$ primary mirror. The test system was similar to the one used at ESO. A small vacuum chamber was mounted at the telescope, placing the pnCCD in the primary focus. With the given focal ratio the angular resolution was about $1''$/pixel. This resulted in a field-of-view of about $4'$. The site of the telescope in the mountains of Crete offers very good observing conditions.

Among the observed objects was the standard object used for high-speed astronomical observations, the Crab Pulsar. It is the collapsed core of a star that ended its life in a supernova explosion which was observed in the year 1054 by Chinese and Arab astronomers. It is surrounded by the Crab Nebula which was also formed by the supernova. The pulsar rotates with a period of roughly $33.602\,\mathrm{ms}$. In figure 12 the nebula is shown in a long-exposure composite colour image composed from three images taken with standard B-, V- and H_α-filters. The whole nebula as seen in the image was also observed without filter at speeds of up to 350 fps and partially with up to 2000 fps. The full frame images with a cycle time of $2.8\,\mathrm{ms}$ were folded with the rotation period of the pulsar and summed

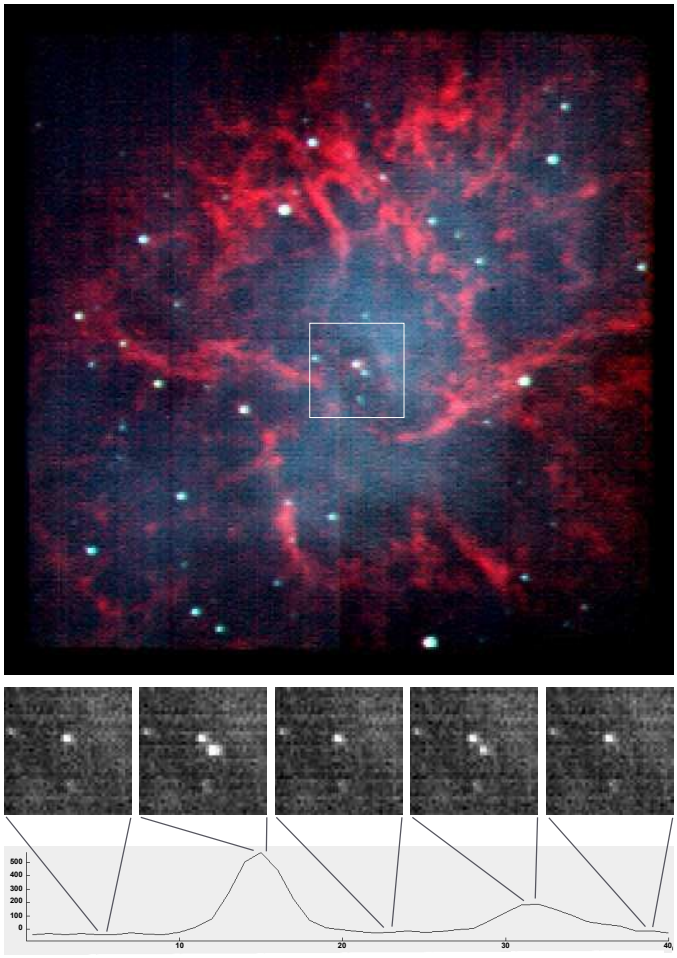

Fig. 12. Top: composite colour image composed from three images taken with standard B-, V- and H_α-filters; middle: detailed views from a 40 frame movie of images with 2.8 ms cycle time; bottom: lightcurve of the movie.

up in 40 bins. All 40 images give a movie of the pulsation of the pulsar. The region marked by the white rectangle is shown for five of these images in the middle of the figure. It can be seen that the "blinking" of the pulsar can be nicely resolved. The lightcurve at the bottom shows the total signal of the pulsar in a circular region of 3 pixels diameter. The background of the nebula is determined from the surrounding pixels and subtracted. The gain used in this measurement is about $10\,^{\mathrm{ADU}}/_{\mathrm{e}^-}$. The pulsars flux in the main peak is only 50 photons in a single frame whereof 20 photons are in the central pixel. The secondary peak with less than 20 photons is also nicely separated from the background.

V. Summary

Optical test measurements have been performed at the optical test bench of ESO in Garching, Germany. The main component of the test system is a fully depleted, backside illuminated pnCCD with 264×264 pixels of 48 µm size. The whole system is optimized for high-speed optical applications. The key feature of the system in that respect is low noise of less than 2.5 electrons ENC at frame rates of up to 1000 fps.

The measured QE is higher than 90 % over a wide wavelength range and peaks at almost 100 %. The in house production at the Semiconductor Laboratory of the Max-Planck-Institutes allows the adjustment of the ARC on the entrance window to match the QE to the needs of a variety of possible applications.

With values as low as 20 µm, corresponding to appreciably less than half a pixel, the measured PSF is very good for a backside illuminated detector of 450 µm thickness. These values are well within the requirements of ESO for future AO systems.

The PTC measurements showed no peculiarities. The nonlinearity for the highest gain was determined to be lower than half a percent. Also the gain showed almost no dependence on the signal level.

We demonstrated the feasibility of a novel fast readout scheme for low light levels that allows full frame readout with up to 1000 fps corresponding to about 70 MHz mean pixel rate without significant decrease in detector performance. As anticipated, PTC measurements in this mode confirmed that signals up to about 6000 electrons per column can be measured with good linearity.

Astronomical test measurements were carried out at the Skinakas telescope on Crete, Greece. The performance was demonstrated with high-speed full frame observations of e.g. the Crab Pulsar. Thereby the operation of the system in a realistic environment could be tested.

Acknowledgment

The authors are grateful to all people involved in the development of our detectors, especially the technology staff of the Semiconductor Laboratory of the Max-Planck-Institutes and PNSensor. Also we want to thank everybody that contributed to this paper.

Finally we want to thank the staff at the Skinakas telescope. They have shown great commitment supporting our measurements.

The project was supported by the Johannes-Heidenhain-Stiftung.

References

[1] L. Strüder, H. Bräuninger, U. Briel, R. Hartmann, G. Hartner, D. Hauff, N. Krause, B. Maier, N. Meidinger, E. Pfeffermann, M. Popp, C. Reppin, R. Richter, D. Stotter, J. Trümper, U. Weber, P. Holl, J. Kemmer, H. Soltau, A. Viehl, and C. V. Zanthier, "A 36 cm^2 large monolithic pn-charge coupled device X-ray detector for the European XMM satellite mission." *Review of Scientific Instruments*, vol. 68, pp. 4271–4274, Nov. 1997.

[2] R. Hartmann, W. Buttler, H. Gorke, S. Herrmann, P. Holl, N. Meidinger, H. Soltau, and L. Strüder, "A high-speed pnCCD detector system for optical applications," *Nuclear Instruments and Methods in Physics Research A*, vol. 568, pp. 118–123, Nov. 2006.

[3] R. Hartmann, "The quantum efficiency of pn-detectors from the near infrared to the soft X-ray region," *Nuclear Instruments and Methods in Physics Research A*, vol. 439, pp. 216–220, Dec. 1999.

[4] A. Karcher, C. J. Bebek, W. F. Kolbe, D. Maurath, V. Prasad, M. Uslenghi, and M. Wagner, "Measurement of Lateral Charge Diffusion in Thick, Fully Depleted, Back-Illuminated CCDs," *IEEE Transactions on Nuclear Science*, vol. 51, pp. 2231–2237, Oct. 2004.

[5] N. Kimmel, J. S. Hiraga, R. Hartmann, N. Meidinger, and L. Strüder, "The direct measurement of the signal charge behavior in pnCCDs with subpixel resolution," *Nuclear Instruments and Methods in Physics Research A*, vol. 568, pp. 128–133, Nov. 2006.